Clim. Past, 10, 1645–1657, 2014
www.clim-past.net/10/1645/2014/
doi:10.5194/cp-10-1645-2014

Climate of the Past
Open Access

Relative impact of insolation and the Indo-Pacific warm pool surface temperature on the East Asia summer monsoon during the MIS-13 interglacial

Q. Z. Yin[1], U. K. Singh[1], A. Berger[1], Z. T. Guo[2], and M. Crucifix[1]

[1]Georges Lemaître Centre for Earth and Climate Research, Earth and Life Institute, Université Catholique de Louvain, 1348 Louvain-la-Neuve, Belgium
[2]Key Laboratory of Cenozoic Geology and Environment, Institute of Geology and Geophysics, Chinese Academy of Sciences, 100029 Beijing, China

Correspondence to: Q. Z. Yin (qiuzhen.yin@uclouvain.be)

Received: 17 January 2014 – Published in Clim. Past Discuss.: 7 March 2014
Revised: 28 June 2014 – Accepted: 24 July 2014 – Published: 1 September 2014

Abstract. During Marine Isotope Stage (MIS)-13, an interglacial about 500 000 years ago, the East Asian summer monsoon (EASM) was suggested exceptionally strong by different proxies in China. However, MIS-13 is a weak interglacial in marine oxygen isotope records and has relatively low CO_2 and CH_4 concentrations compared to other interglacials of the last 800 000 years. In the meantime, the sea surface temperature (SST) reconstructions have shown that the warm pool was relatively warm during MIS-13. Based on climate modeling experiments, this study aims at investigating whether a warmer Indo-Pacific warm pool (IPWP) can explain the exceptionally strong EASM occurring during the relatively cool interglacial MIS-13. The relative contributions of insolation and of the IPWP SST as well as their synergism are quantified through experiments with the Hadley Centre atmosphere model, HadAM3, and using the factor separation technique. The SST of the IPWP has been increased based on geological reconstructions. Our results show that the pure impact of a strong summer insolation contributes to strengthen significantly the summer precipitation in northern China but only little in southern China. The pure impact of enhanced IPWP SST reduces, slightly, the summer precipitation in both northern and southern China. However, the synergism between insolation and enhanced IPWP SST contributes to a large increase of summer precipitation in southern China but to a slight decrease in northern China. Therefore, the ultimate role of enhanced IPWP SST is to reinforce the impact of insolation in southern China but reduce its impact in northern China. We conclude that a warmer IPWP helps to explain the strong MIS-13 EASM precipitation in southern China as recorded in proxy data, but another explanation is needed for northern China.

1 Introduction

Marine Isotope Stage (MIS)-13, an interglacial about 500 ka ago, is the coolest interglacial of the past 800 ka over Antarctica (Jouzel et al., 2007). The average CO_2 concentration is about 240 ppmv, which is low for an interglacial (Luthi et al., 2008). It also has higher marine benthic $\delta^{18}O$ values than other interglacials, implying larger continental ice sheets and/or cooler deep-sea temperature. However, the paleosoil S5-1 in the loess from northern China, which corresponds to MIS-13, is the strongest developed soil of the past 800 ka, suggesting extremely strong East Asian summer monsoon (EASM) precipitation (e.g., Kukla et al., 1990; Guo et al., 1998). This strong EASM was confirmed by the lake sediments from the Tibet Plateau (Chen et al., 1999) and by the paleo-red-soils from southern China (Yin and Guo, 2006). It appears also as strong as the other interglacials in the stalagmite records from western China (Cheng et al., 2012). These terrestrial reconstructions are in line with maritime summer monsoon proxy (Wei et al., 2007) and sea surface salinity reconstruction (Shyu et al., 2001) in the South China Sea. A strong EASM occurring during a relatively cool

interglacial MIS-13 was pointed out by Yin and Guo (2008) as a seeming paradox.

In order to understand this seeming paradox, several modeling studies have investigated the impacts of insolation and ice sheets on the MIS-13 EASM. Using the LOVECLIM model (an Earth system model of intermediate complexity), Yin et al. (2008, 2009) found that strong summer insolation in the Northern Hemisphere (NH) contributes to intensify the EASM during MIS-13 as compared to today, but insolation alone does not make the MIS-13 EASM exceptionally strong as compared to other interglacials. Unexpectedly, they also found that a small Eurasian ice sheet reinforces additionally the EASM through a topographically induced wave train, which might explain the exceptional EASM during MIS-13. These findings have been confirmed by more complex general circulation models including an atmosphere-only model ARPEGE (Sundaram et al., 2012; Muri et al., 2012) and an atmosphere–ocean coupled model HadCM3 (Muri et al., 2013). However, it is still unclear if there was any other ice sheet than Greenland in the NH during MIS-13 because some terrestrial proxies seem to indicate a relatively warm condition during this interglacial (Guo et al., 2009). This means that the explanation provided by the Eurasian ice sheet for an exceptional MIS-13 EASM becomes uncertain, and other factors might play a role.

Recently, hydrographic reconstructions from the South China Sea suggest that the tropical dynamics would have played a role in the climate abnormality during MIS-13 through maintaining or even increasing the longitudinal sea surface temperature (SST) gradient in the equatorial Pacific (Yu and Chen, 2011). Although MIS-13 was cooler than most of the interglacials over most of the oceans (Lang and Wolff, 2011), SST reconstructions from the western Pacific warm pool region (Medina-Elizalde and Lea, 2005; de Garidel-Thoron et al., 2005) show that this region during MIS-13 is as warm as or warmer than many other interglacials. The maximum annual mean SST reconstruction during MIS-13 of de Garidel-Thoron et al. (2005) (2°2′ N, 141°46′ E) is about 1 °C higher than today (29.46 °C).

The Indo-Pacific warm pool (IPWP) is an important feature of the climate system. Through the excitement of atmospheric deep convection, the warm pool is capable of influencing global climate via the Walker and Hadley circulations and serves as a major source of heat and water vapor (Sardeshmukh and Hoskins, 1988; Webster and Lukas, 1992). This warm pool is a major source of moisture for the Asian summer monsoon. The SST anomalies there have been considered to be important for monsoon variability (Nitta, 1987; Shen and Lau, 1995; Lau et al., 2000; Kawamura et al., 2001). The warming of IPWP has caused rainfall to increase over most of the local basin and the maritime continent (Zhou et al., 2009). Many studies (e.g., Nitta, 1987; Kurihara, 1989; Huang and Sun, 1992) have shown that the thermal state of the tropical western Pacific and convective activity around the Philippines play important roles in the interannual variability of EASM. Lu (2001) also showed that the convective activity over the tropical western Pacific plays a key role in modulating the strength and displacement of the western Pacific subtropical high (WPSH) which has in turn a strong influence on East Asia summer monsoon variability. According to Zhao et al. (2000), if the western tropical Pacific warm pool temperature increases, the subtropical high extends further westward in the northwest Pacific Ocean, and its ridge is displaced further southward, resulting in a change of the precipitation pattern in China. Moreover Zhou et al. (2009) explored the impacts of higher and lower pool SSTs on the East Asia summer monsoon rainfall for the present day using five different atmospheric general circulation models. Their results suggest that the SST changes in the warm pool influence the Walker circulation, with a subsequent reduction of convection in the tropical central and eastern Pacific, which in turn forces an El Niño–Southern Oscillation (ENSO)/Gill-type response that modulates the WPSH.

Given the importance of the IPWP SST on the EASM and the enhanced SST in the warm pool region during MIS-13, one may wonder which role this warm pool warming plays on the EASM during MIS-13, whether it is at the origin of the exceptionally strong EASM during this interglacial, and what its relative importance is as compared to insolation. We aim at answering these questions in this study by performing sensitivity experiments with the Hadley Centre atmosphere model HadAM3. The individual impacts of the IPWP warming and of insolation, as well as their synergism, are quantified through factor separation analysis (Stein and Alpert, 1993) (see Sect. 2 for detailed information). Although many studies have discussed the impact of warm pool surface conditions on the EASM (see the paragraph above), they are mainly based on modern background climate and insolation. Given the different configurations in the climate forcings (for example, NH summer occurs at aphelion at present day, but it may occur at perihelion during the past interglacials), it is worth investigating the impact of warm pool during the past interglacials using climate models. Moreover, factor separation analysis allows separating the pure impact of insolation and of the warm pool warming as well as their synergism. Therefore, this study may provide broader implications than only for MIS-13 regarding the impact of warm pool warming on the EASM and its synergic effect with insolation.

The EASM system is generally described as the combination of three main components: the East Asian *meiyu*/*baiu*/*changma* front (a major rain-bearing system in the subtropics and mid-latitudes), the western Pacific subtropical high, and the tropical western Pacific monsoon trough, which corresponds to the western Pacific intertropical convergence zone (ITCZ). In addition, the intensity and location of subtropical westerly jet (SWJ) and tropical easterly jet (TEJ) at upper level (200 hPa), and the modulation of the Hadley and Walker circulations play a major role in the EASM rainfall variability. These EASM-associated features are analyzed here. In this study, East China monsoon region

Table 1. Experiment list. "MIS-13" insolation means the insolation at 506 ka BP. "MIS-13" SST means the simulated MIS-13 SST by Muri et al. (2013) using the atmosphere–ocean coupled model HadCM3 forced by the MIS-13 insolation and greenhouse gas concentrations. "Warmer warm pool" SST is the same as "MIS-13" SST except that the SST over the IPWP is increased. Detailed information about forcing and boundary conditions is given in Sect. 2.

Experiment name	Insolation	SST
f_{00}	Present	MIS-13
f_{10}	MIS-13	MIS-13
f_{01}	Present	warmer warm pool
f_{11}	MIS-13	warmer warm pool

refers to the area between 105–120° E and 20–40° N (Wei and Wang, 2004; Lee et al., 2008), northern and southern China being separated by 30° N latitude. Model and experiment design are given in Sect. 2. The pure impacts of insolation and of the IPWP SST enhancement on the EASM, their synergism as well as their combined effect are discussed in Sect. 3. Conclusion is given in the final section.

2 Model and experiment design

As we would like to investigate the impact of enhanced warm pool SST on the EASM during MIS-13, SST is prescribed in our experiments. In such a case, an atmosphere-only model instead of an atmosphere–ocean coupled model is required. The atmosphere model used here is HadAM3 (Pope et al., 2000), which was developed at the Hadley Centre for Climate Prediction and Research. It is based on the hydrostatic and primitive equations and uses an Arakawa B-grid and hybrid vertical coordinates. It has a horizontal resolution of 3.75° in longitude and 2.5° in latitude, with 19 vertical levels. HadAM3 has been demonstrated to perform well in the atmospheric model intercomparison project and to produce a reasonable representation of the Asian monsoon circulations and precipitation (Martin et al., 2000; Zhou et al., 2009). It has also been used in many studies on the response of East Asian monsoon to modified forcings. For example, Liu et al. (2012) have recently used HadAM3 to investigate the impact of the changes in Tibetan Plateau thermal forcing on the EASM.

As far as the methodology used is concerned, we stress that, different from the traditional studies where sensitivity experiments are made to investigate the impact of only one factor (insolation or SST), in this study we would like to test the relative importance of insolation and of the warm pool SST on the EASM. In the traditional studies where the impact of only one factor is evaluated, the common procedure is to analyze the difference between a control run and a simulation where this factor is switched off. However, this difference between two experiments does not have a simple meaning when more than one factor are involved, because it includes the pure impact of one factor and the joint effect (or synergism) with all the other factors. In the case of more than one factor, the Alpert–Stein factor separation methodology (Stein and Alpert, 1993) must therefore be used because it allows isolating the individual effect of each factor on any climatic variable as well as the synergistic effect with the other factors. This methodology has been used in many modeling studies to quantify the relative importance of specific processes or forcings and their interactions as, for example, for the Holocene (Berger, 2001; Claussen et al., 2001), the Eemian (Kubatzki et al., 2000; Crucifix and Loutre, 2002) and the last nine interglacials (Yin and Berger, 2012).

In this study, the Alpert–Stein factor separation methodology is applied to two factors: the warm pool SST and insolation. This requires four experiments (Table 1) to be made which are labeled 00, 01, 10 and 11 for any climatic variable, f. The simulated field will be given the value f_{11} when all factors are acting, and a value f_{00} when they are all "switched off". In the other two experiments, f_{10} and f_{01}, only one factor is changed at a time. According to Stein and Alpert (1993), we have

$$f_{11} = f_{00} + \widehat{f_{10}} + \widehat{f_{01}} + \widehat{f_{11}}, \quad (1)$$

where $\widehat{f_{10}} = f_{10} - f_{00}$ is the pure contribution of insolation; $\widehat{f_{01}} = f_{01} - f_{00}$ is the pure contribution of enhanced warm pool SST; $\widehat{f_{11}} = f_{11} - f_{00} - \widehat{f_{10}} - \widehat{f_{10}}$ is the synergism between insolation and warm pool SST.

The reference insolation and reference SST (Table 1) are respectively the present-day insolation and the 12-month SST simulated by the atmosphere–ocean coupled model HadCM3 forced by the MIS-13 insolation and greenhouse gas concentrations (Muri et al., 2013). They have been used in the reference experiment f_{00}. In the experiment f_{10}, the insolation of MIS-13 and the reference SST are used. In the experiment f_{01}, the reference insolation and the modified SST are used. As the IPWP is typically defined as the oceanic region enclosed by the 28 °C isotherm of SST (e.g., Ho et al., 1995; Fasullo and Webster, 1999) and as it appears particularly warm from March to July with the highest peak in May (Zhang et al., 2009), the modified SST is obtained by adding 1 °C to the reference SST from March to July at each grid point of the IPWP region (where SST $\geq$ 28 °C or the great warm pool) which extends from the eastern equatorial Indian Ocean to the western tropical Pacific (Fig. 1). Based on some available studies (Zhou et al., 2009; Li et al., 1999; Zhao et al., 2000), it could be said that the EASM regional precipitation is very sensitive to changes in SST over the warm pool region at the seasonal and annual scales. We note that, due to lack of precise reconstruction of the warm pool SST during MIS-13 at these scales, this change in SST is used only as a sensitivity test. In the control experiment f_{11}, the MIS-13 insolation and the modified SST are used. Therefore, the pure impact of insolation, of increased IPWP SST, their synergism

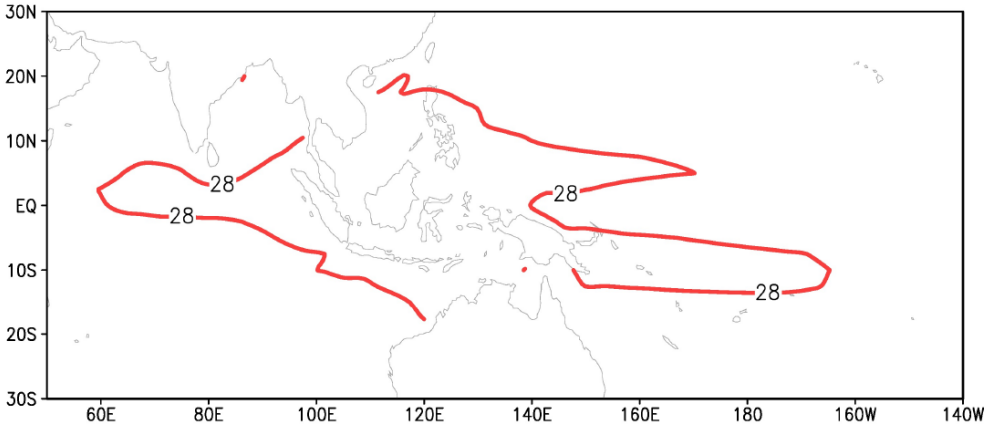

Figure 1. Area of the Indo-Pacific warm pool surrounded by 28 °C isotherm line. Annual mean SST values are provided by the HadCM3 simulation for MIS-13 (Muri et al., 2013).

and their combined impact are given by $f_{10} - f_{00}$, $f_{01} - f_{00}$, $f_{11} + f_{00} - f_{10} - f_{01}$, and $f_{11} - f_{00}$, respectively. We note that, due to the difference in methodology between our study where the impacts of both insolation and SST are evaluated at the same time (using the factor separation methodology) and the traditional study where only one factor is evaluated for a given specific value of the other factor, we must be cautious when comparing our results with those from the traditional study.

Snapshot simulations have been made like in many paleoclimate modeling studies. The same greenhouse gas concentrations and astronomical parameters as in previous MIS-13 simulations (Yin et al., 2008) have been used. All four experiments use the same greenhouse gas concentrations (CO_2 equivalent = 240 ppmv). The insolation of MIS-13 was calculated according to the astronomical parameters at 506 ka BP (Berger, 1978). The large eccentricity and NH summer occurring at perihelion lead to more insolation received by the whole earth but particularly over the NH during boreal summer. For each experiment, the model is integrated over 35 years, but only the data obtained over the last 10 years are analyzed.

3 Results and discussions

In this section, the pure contributions to the MIS-13 EASM of insolation and of enhanced IPWP SST are analyzed, as well as their synergism and combined effects.

3.1 Pure contribution of insolation on the EASM

As can be seen from Fig. 2a, the summer temperature anomalies due to insolation change only ($f_{10} - f_{00}$) over the NH continents are positive. The maximum summer temperature anomaly reaches 6 °C over the mid-latitude land. This increase in temperature over land combined with the lack of temperature increase over the ocean results in a stronger land–sea thermal contrast. Chou (2003) showed that strong meridional temperature gradient due to land–sea heating contrast enhances the intensity of Asian summer monsoon and extends the corresponding monsoon rain belt northeastward. Correspondingly, the low pressure over the Asian continent becomes deeper, and the high pressure over the Pacific and Indian Ocean is intensified. The intensified and northward-shifted high-pressure system over the northwestern Pacific contributes to the strengthening and northward displacement of the EASM rain belt over northern China via changes in the low-level prevailing winds.

Under the impact of insolation only, a huge increase in JJA precipitation (2.4 mm day^{-1}) is simulated over northern China but a very small change over southern China (Fig. 3). The spatial distribution of summer precipitation anomalies (Fig. 4a) shows a significantly drier condition over Indo-China and south of the Indian Peninsula but wetter conditions in northern China, northeast Asia, northern India and south of Tibet. Increase in JJA precipitation over northern China and northeast Asia is due to the large warming over the NH land with an enhanced land–sea thermal contrast and a shifting of ITCZ to the north. The ITCZ can be indicated by the strongest rising motion in the Hadley cell (Fig. 5a). Under the influence of insolation, there is an anomalous descending motion around 20° N and an anomalous rising one around 35° N, indicating a northward movement of the ITCZ (Fig. 5b). Another important atmospheric feature for the East Asian summer monsoon is the East Asian jet, which is jointly controlled by extratropical dynamics and tropical heating. The changes in position and intensity of the jet core is directly associated with the meridional gradient of air temperature in the troposphere (the larger the meridional gradient, the stronger the jet). The East Asia jet displacement has a large impact on the position of the monsoon rain belt over East Asia especially in summer (e.g., Liang and Wang, 1998; Kuang and Zhang, 2006). Indeed, under the impact of insolation only, the area of maximum temperature gradient shifts

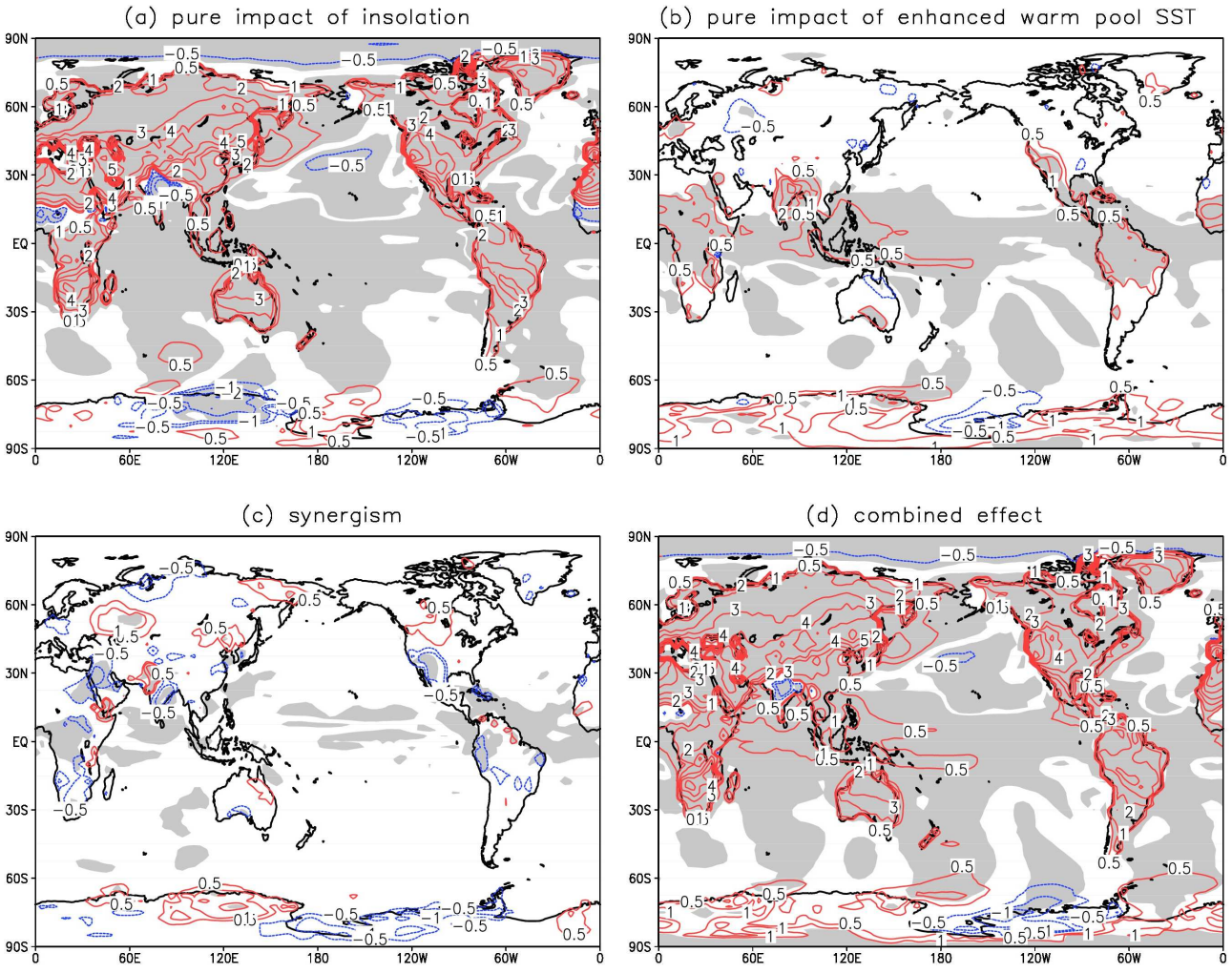

Figure 2. Simulated summer (JJA) surface air temperature anomaly (°C). **(a)** Pure impact of insolation, **(b)** pure impact of enhanced IPWP SST, **(c)** synergism between insolation and enhanced IPWP SST and **(d)** combined effect of insolation and enhanced IPWP SST. Areas with significance level greater than 99 % are shaded in gray.

north due to a northward displacement of the maximum heating over the northern continents in the upper level. As indicated by the zonal wind anomaly at 200 hPa, Fig. 5b shows that the southern part of the subtropical East Asian jet is significantly weakened and its northern part is intensified and expanded. This is accompanied by a strong anomalous rising motion over northern China providing more rainfall there.

For more details about ascending and descending motions over East Asia, the vertical velocity (omega) has been analyzed. The JJA vertical velocity anomaly shows a strong ascending motion occurring between 30 and 40° N from the surface to upper level (Fig. 7a) and leading to more precipitation through deep convection over northern China (as shown also by the meridional wind circulation anomaly in Fig. 5b). Under the impact of insolation only, the ITCZ and East Asian jet both shift northward from their mean position, while a strong low-level convergence dominates the region near 35° N, all phenomena related to the rain associated with the *meiyu*/*baiu*/*changma* front. The enhanced land–sea thermal contrast and enhanced meridional temperature gradient during boreal summer strengthens the EASM circulation, leads to stronger southerly winds prevailing over eastern China and finally to more northward transport of water vapor (Fig. 8a) from the Arabian Sea, the Bay of Bengal and the western Pacific. Figure 8a shows that, under the impact of high NH summer insolation, the Arabian Sea and the Bay of Bengal are important sources of moisture transport to southern China, but in northern China moisture originated from the western Pacific.

The seasonal cycle of precipitation anomaly shows over northern China an increase from March to June with a plateau in July (2.8 mm day^{-1} in June and in July) and a sharp decrease from August and September. This is generally in phase with seasonal changes in local surface temperature and inso-

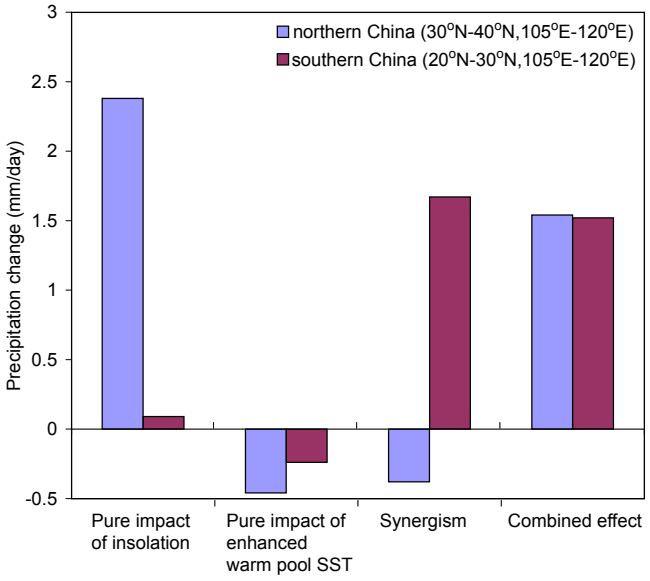

Figure 3. Summer precipitation change averaged over northern and southern China.

lation, showing the importance and direct influence of these factors on the northern EASM precipitation. Over southern China there is an abrupt increase only from April to May ($2.5\,\mathrm{mm\,day^{-1}}$) and decrease from May to June (Fig. 6a, b). This is completely independent of local insolation and temperature changes, indicating the influence of the internal feedbacks in particular from the insolation-driven seasonal SST changes on the southern EASM precipitation. Shi et al. (2012) show that the condition of the tropical Pacific SST can modulate the impact of insolation leading to different response of the EASM precipitation to insolation in northern and southern China. The general features of our insolation-induced changes in atmospheric circulations and regional precipitation patterns are in line with the results of other modeling studies (Wei and Wang, 2004; Braconnot et al., 2008), showing the robustness of the model response to modified insolation forcing.

3.2 Pure contribution of the IPWP SST on the EASM

The pure impact of enhanced IPWP SST ($f_{01} - f_{00}$) leads to a slight decrease in JJA precipitation in both northern and southern China (Fig. 3). The spatial distribution of the summer precipitation anomalies (Fig. 4b) shows a drier condition over India and China but a wetter one over the IPWP region itself and over the maritime continents. It indicates that the SST increase over the IPWP region only leads to an increase in local convection and precipitation, but reduces the EASM precipitation. Such a warmer IPWP reduces the land–sea thermal contrast over the NH land in summer and shifts the ITCZ southward as indicated by the change in the meridional wind circulation anomaly (Fig. 5c). Here, the 200 hPa subtropical jet also shifts southward as indicated by the change in the zonal wind circulation anomaly (Fig. 5c), leading to more rainfall over East Asia south of 20° N. The remarkable decrease in the land–sea thermal contrast during boreal summer weakens the EASM circulation and generates northerly wind anomaly over eastern China, which prevents the northward transport of water vapor as shown in Fig. 8b. The vertical velocity anomaly (Fig. 7b) indicates that the ascending motion over $\sim 30°$ N almost disappears, being changed into a weak descending motion over both northern and southern China from the surface to the upper levels revealing less convection and precipitation over the whole of China. On the contrary, anomalous ascending motion occurs south of 20° N along with precipitation increase due to stronger local convection caused by the enhancement of the IPWP SST. We note that an atmosphere-only model is used in our study. This means that there is no feedback from atmosphere to ocean. Duan et al. (2008) found that the atmospheric feedbacks cool SST through enhanced evaporation and reduced solar heating caused by deep convection during the active phase of monsoon. They found that absence of such kinds of feedbacks in the atmosphere-only model generates more precipitation over the IPWP by maintaining the high SST for too long. According to their study, the large precipitation increase over the IPWP in our study might therefore be exaggerated.

Our simulated result that increased SST over the IPWP leads to reduced summer precipitation in China is in line with other modeling studies. By using a two-level global circulation model, Huang and Sun (1992) showed that when the SST over tropical western Pacific warm pool is above normal, then East Asia receives below normal rainfall in summer. Tschuck et al. (2004) also showed that a warmer western Pacific leads to anomalous north-easterlies over China indicating a weakened East Asian monsoon.

Many studies have used modern observational data or proxy reconstructions to discuss the relationship between SST and the precipitation in China, but interpretations based on data are much more diverse than based on modeling results. Zhao et al. (2000) found that increased SST in the western Pacific warm pool corresponds to less rainfall in northern China and more rainfall in southern China. Zhang et al. (2009) studied the correlation between the western Pacific warm pool SST and the East China precipitation during the past 360 years. They found that this correlation has strong regional diversity, but it is only over the Yellow River and Huaihe River basin in northern China that this correlation (negative) is significant. Yang and Lau (2004) found that the interannual variation of the summer precipitation over central eastern China and over southern coastal China is correlated with a north–south dipole mode of SST anomalies over the western North Pacific, the tropical Indian Ocean and the warm pool: when SSTs are abnormally warm over the warm pool and northern Indian Ocean and are abnormally cold over the western North Pacific, summer precipitation tends to be heavier than usual in central eastern China but to be less in

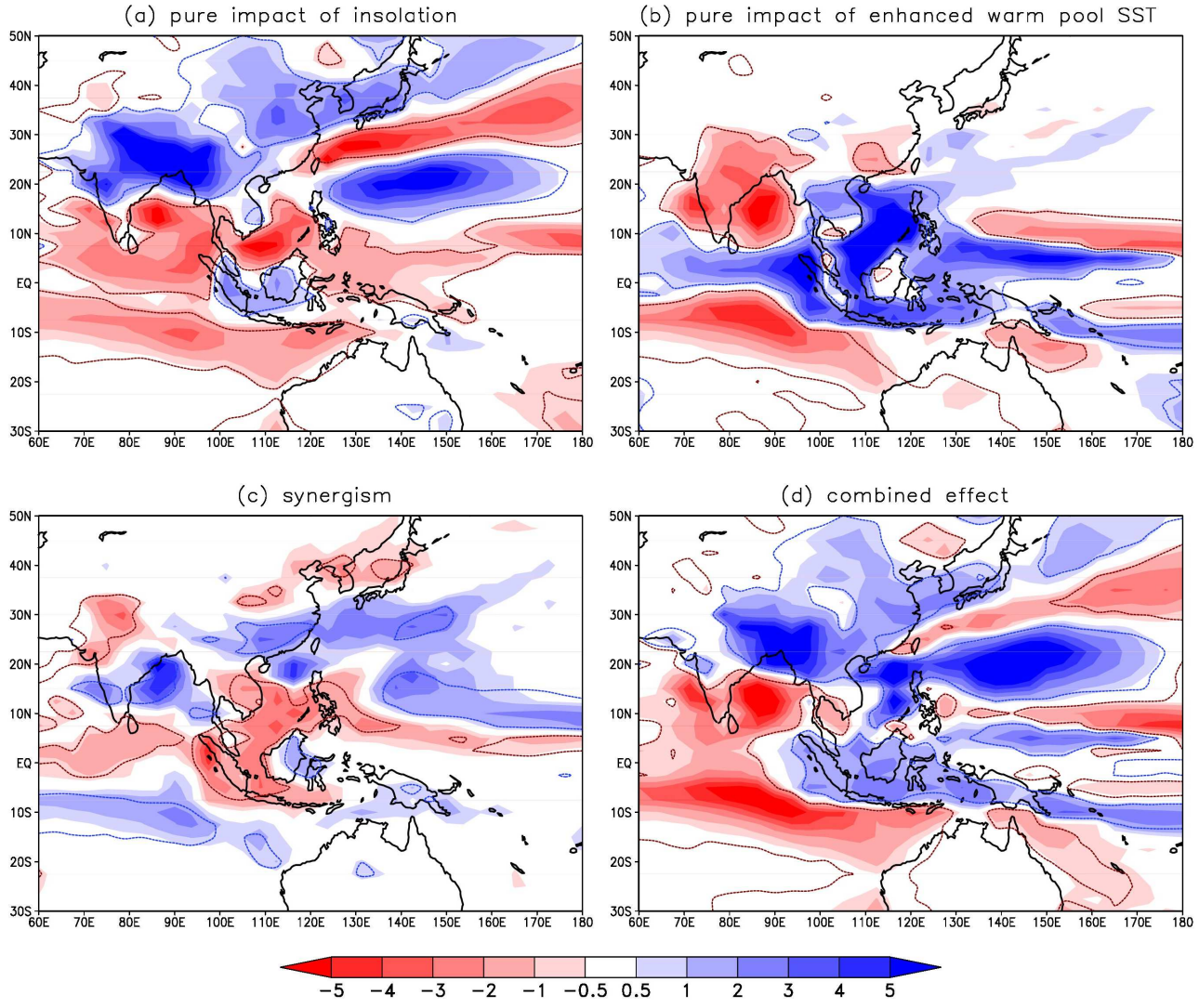

Figure 4. Same as Fig. 2 except for summer precipitation anomaly (mm day^{-1}). Areas with significance level greater than 99 % are surrounded by contour lines.

southern coastal China. Lee et al. (2008) found that the north EASM precipitation is negatively correlated with the tropical western Pacific SST and is positively correlated to the tropical Indian Ocean SST, and that the south EASM precipitation is positively correlated with the western North Pacific SST but has no obvious correlation with the Indian Ocean SST. However, also based on observational data, Saji and Yamagata (2003) found that the precipitation over India and southern China is enhanced during the positive IOD (Indian Ocean dipole) event, an event which is characterized by anomalous cooling in the eastern equatorial Indian Ocean and anomalous warming in the western equatorial Indian Ocean.

The different findings from these studies based on data or proxy reconstructions might be related to different data sets or different analytical techniques which have been used. Nevertheless, these studies tend to show that the summer precipitation in northern China is negatively correlated with the SST in the western Pacific warm pool, which is in agreement with our model results. The conclusions are more controversial for southern China. Among them, Zhao et al. (2000) found a positive correlation between southern China precipitation and the SST of western Pacific warm pool. This, at a first glance, seems to be contrary to our results, but actually it is not because it is not appropriate to compare the finding of Zhao et al. (2000) with our results. In our experiment the SST is indeed enhanced not only over the western Pacific warm pool but also over the Indian Ocean warm pool, a region extending from the tropical western Pacific to the eastern equatorial Indian Ocean (Fig. 1). This means that in our simulation the precipitation in southern China responds to changes in SST not only in the western Pacific warm pool but also in the Indian Ocean warm pool. In our experiment, due

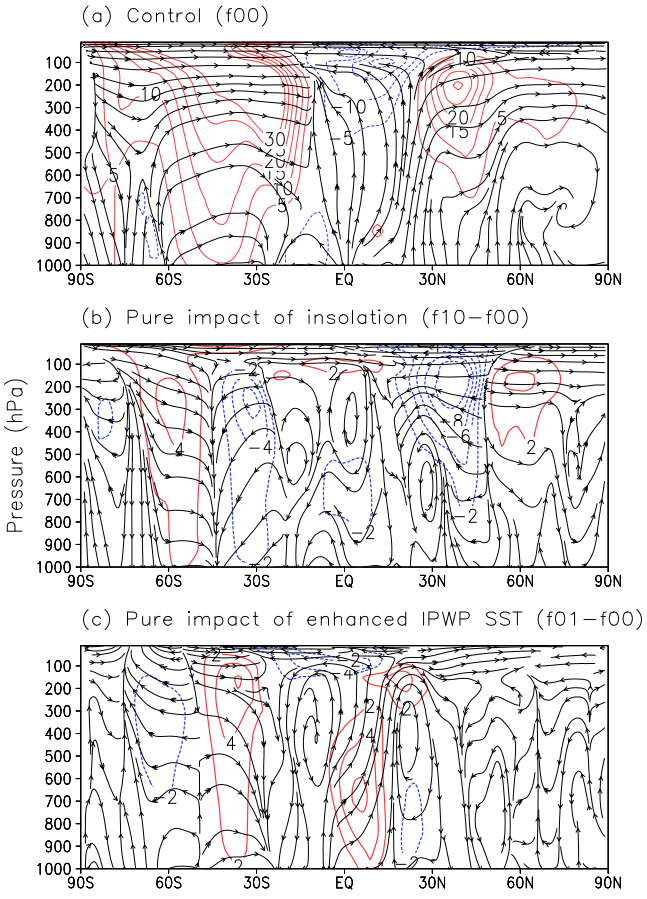

Figure 5. JJA mean meridional wind circulations averaged over 105 to 120° E. **(a)** The control experiment (f_{00}), **(b)** the pure impact of insolation ($f_{10} - f_{00}$), and **(c)** the pure impact of enhanced IPWP SST ($f_{01} - f_{00}$). Stream lines indicate meridional wind circulation for **(a)** and anomalies for **(b)** and **(c)**. Contour lines indicate zonal wind circulation (with an interval of $5\,\mathrm{m\,s^{-1}}$ for **a**) or anomalies (with an interval of $2\,\mathrm{m\,s^{-1}}$ for **b** and **c**).

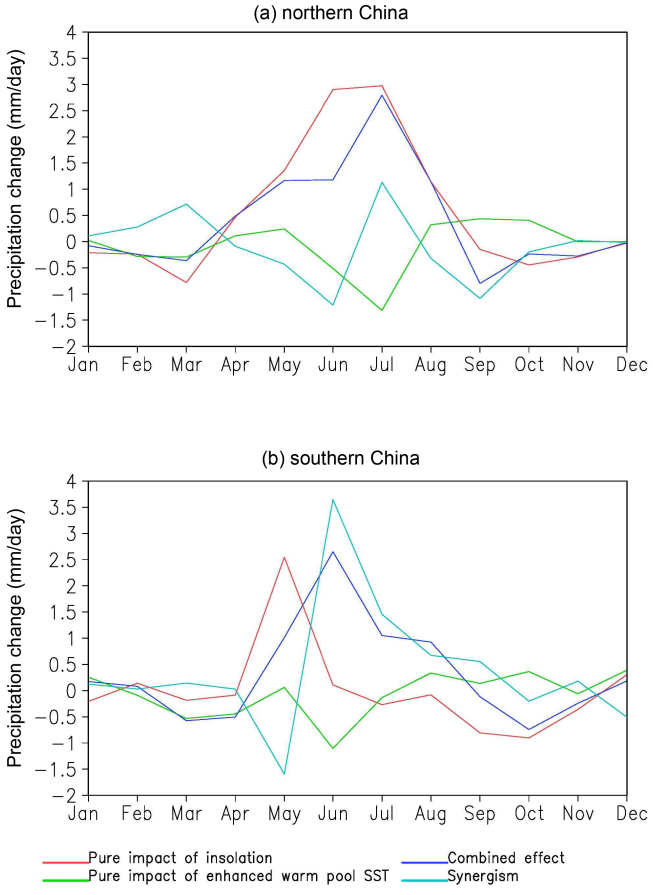

Figure 6. Seasonal cycle of precipitation anomaly over northern **(a)** and southern **(b)** China. Contributions of insolation, of enhanced IPWP SST, their synergism and combined effect are given.

to the SST increase in the eastern equatorial Indian Ocean, a negative "IOD-like" event is created. Presumably opposite to the positive IOD situation as in Saji and Yamagata (2003), a negative IOD might be associated with reduced precipitation over India and southern China, which is indeed the case in our simulation (Fig. 4b).

3.3 Synergism

Synergism can be defined as the additional contribution due to two or more factors when they act together compared to the sum of their individual contributions. It is therefore given by $(f_{11} - f_{00}) - (f_{10} - f_{00}) - (f_{01} - f_{00})$ (see Sect. 2). As shown in Fig. 3, the synergism between insolation and the increase of the IPWP SST contributes to a large increase in the summer precipitation over southern China but decrease over northern China. The corresponding spatial distribution of summer precipitation anomalies due to the synergism (Fig. 4c) shows a drier condition over northern China and northeastern Asia but a wetter over India (west coast of India and north part of Bay of Bengal) and southern China. Consistently, a strong ascending motion is seen in southern China and a weak descending motion in northern China (Fig. 7c). The strong upward motion in southern China corresponds well to the enhanced precipitation there. The EASM circulation is weakened with anomalous northerly winds over eastern China. Such an anomalous northerly surface wind is not favorable for the moisture transport up to northern China. But at the same time, the monsoon circulation over the Indian domain (land and ocean) becomes intensified, providing more moisture transported to southern China (Fig. 8c). In southern China, the synergism can be explained by the intensified meridional transport of water vapor inland over southern China which results from a joint effect of the insolation-induced increased southerly wind and the SST-induced increased local evaporation over the IPWP which provides more water vapor to be transported. These two factors act together providing a better condition for precipitation increase in southern China than when one of them acts alone. In

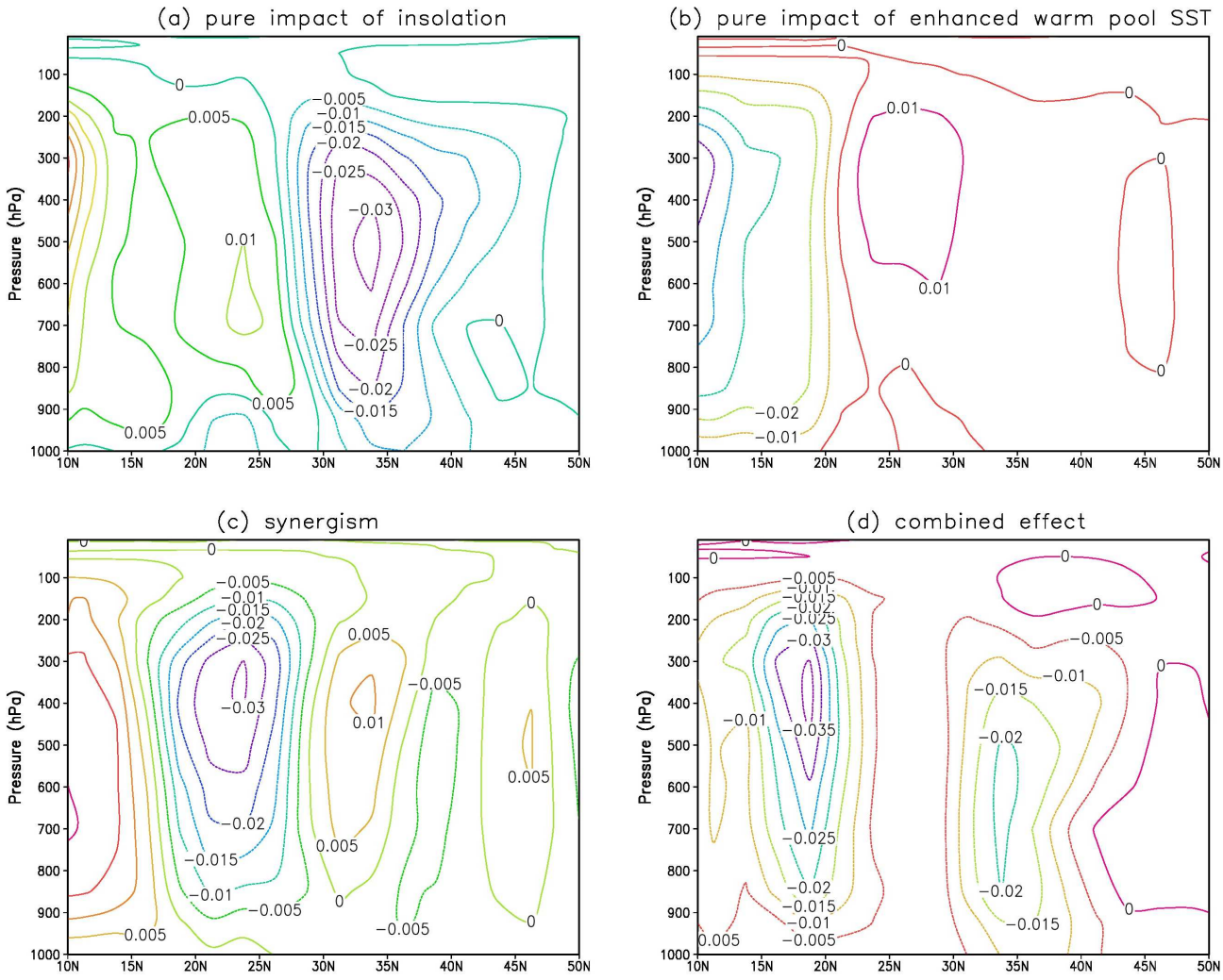

Figure 7. Same as Figs. 2 and 4 except for summer vertical velocity anomaly (Pa s^{-1}) averaged over 105 to 120° E.

vertically integrated moisture transport, a localized cyclonic (moisture convergence) flow over East China could be associated with more precipitation in southern China and less in northern China (Fig. 8c).

3.4 Combined effect of insolation and the IPWP SST and their relative importance

The primary source of monsoon circulation depends largely on the surface latitudinal temperature distribution over land and the adjacent sea especially over the Asian domain. The combined effect ($f_{11} - f_{00}$) of insolation and enhanced SST over the IPWP region decreases the latitudinal temperature gradient at least by 0.5 °C when compared to the pure insolation effect (Fig. 2d compared to Fig. 2a) due to the additional warming over the IPWP region. The combined effect leads to same amount of summer precipitation increase in northern and in southern China (Fig. 3). This is also shown in the spatial pattern of JJA precipitation anomaly (Fig. 4d). Figure 3 shows that the precipitation increase in northern China is only due to changes in insolation whose effect is nevertheless weakened by the effect of enhanced IPWP SST and the synergism. However, the precipitation increase in southern China is mainly due to the synergism, the pure impacts of insolation and of the IPWP SST being quite small. The pure impact of enhanced IPWP SST has relatively small impact over the mainland of China.

The JJA vertical velocity anomaly (Fig. 7d) shows two centers of ascent and deep convection. One is over northern China and results from the pure impact of insolation (Fig. 7a). Another is over southern China and its position indicates that it is mostly contributed from the synergism (Fig. 7c). The heavy rainfall increase in China is closely related to these two strong upward motions. At low level, wind strength and direction during JJA also well support the moisture transport over East Asia from the Indian Ocean and the northwestern Pacific. Analysis of the spatial distribution of

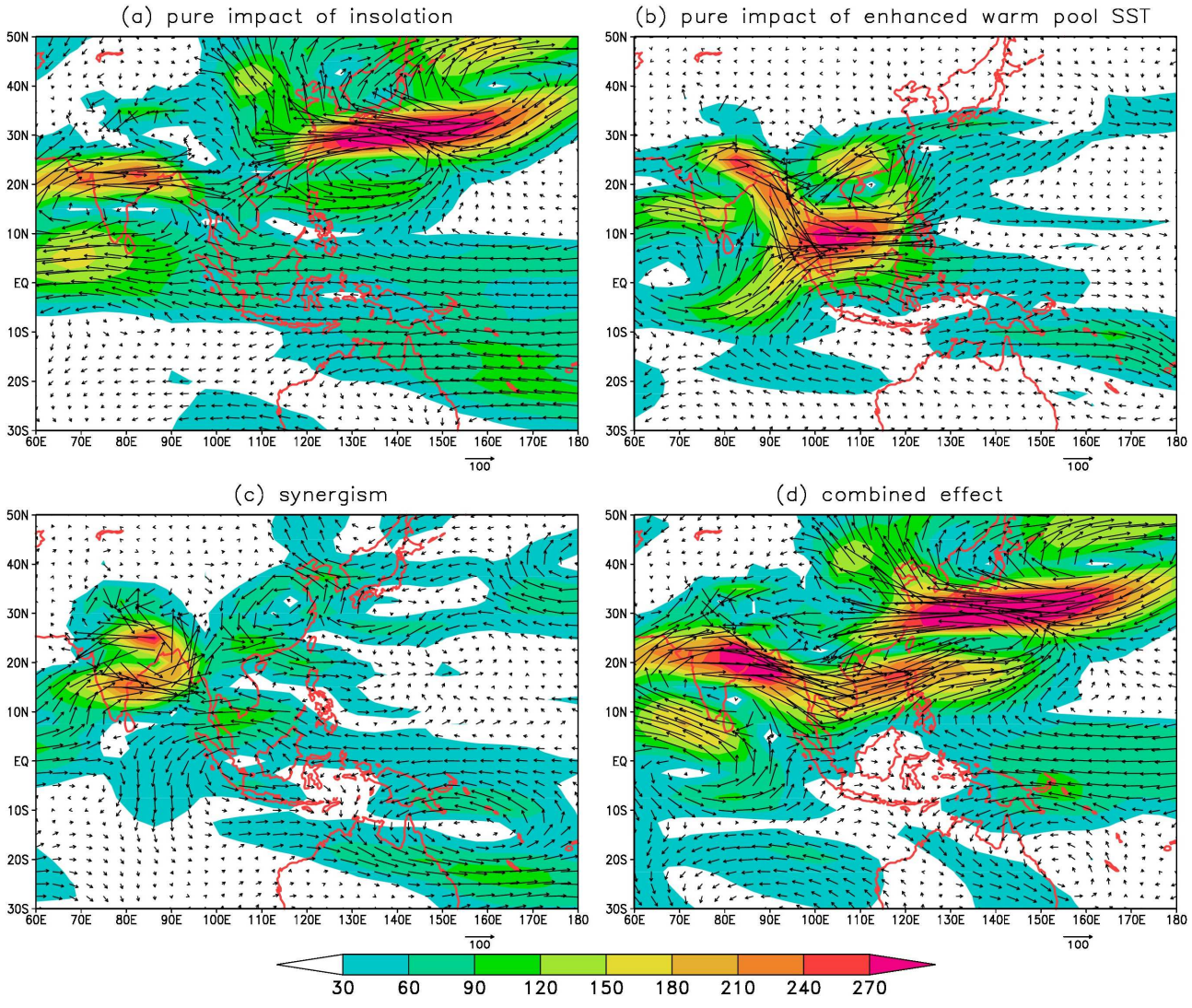

Figure 8. Same as Figs. 2, 4 and 7 except for summer vertically integrated moisture transport anomaly ($\mathrm{Kg\,m^{-1}\,s^{-1}}$) in the whole troposphere.

the total moisture transport (Fig. 8d) shows that, in southern China, the moisture transport is mainly from the Indian Ocean (especially from the Bay of Bengal), and it results from the pure impact of insolation (Fig. 8a) and is reinforced by the synergism effect (Fig. 8c). In northern China, the moisture transport from the west Pacific Ocean dominates, and it completely results from the pure impact of insolation. This, again, shows the dominant role of insolation on the northern EASM precipitation and its joint effect with synergism on the southern EASM precipitation.

For the annual cycle, the precipitation change due to combined effect shows a positive anomaly from April to August with a peak in July for northern China and from May to August with a peak in June for southern China (Fig. 6a, b). In northern China, there is a steep drop from July to September and a more gentle rise from March to July with a plateau in May to June. This plateau is actually due to the fact that a decline of precipitation induced by the pure effect of the enhanced IPWP SST and of the synergism counteracts the increase caused by the pure impact of insolation. In northern China, the peak related to insolation coincides with the peak of the synergism and the deepest minimum in the IPWP SST contribution. This leads to the peak of the combined effect occurring in July. Then there is a fast decline from July to September mainly caused by changes in insolation. In southern China it is quite different with a steep rise from April to June and a more gentle drop from June to October (Fig. 6b). The occurrence of the peak of the combined effect is in June coinciding with the peak of the synergism which appears 1 month later after the peak of the pure effect of insolation. The smooth decrease from July to October is mainly caused by the synergism.

4 Conclusions

Our model results show that strong summer insolation during MIS-13 strengthens the summer monsoon precipitation in both northern and southern China, and particularly in northern China. High summer insolation leads to a large warming over the NH land during its summer, an enhanced land–sea thermal contrast, a northward shift of the ITCZ, an intensification and northward shift of the tropical easterly jet. The northward shift of WPSH, strong low-level southerly wind, more moisture transport from northwest Pacific and South China Sea and strong convection over mid-northern China are observed. The pure impact of enhanced IPWP SST slightly reduces the summer precipitation in both northern and southern China through reducing the land–sea thermal contrast. It however leads to huge precipitation increase over the IPWP region due to strong convection there. The synergism between insolation and enhanced IPWP SST contributes to a large increase of summer precipitation over southern China but to a decrease in northern China. Finally, the combined effect of insolation and enhanced IPWP SST leads to EASM precipitation increase in both northern and southern China.

Our model results show that the increase of EASM precipitation in northern China during MIS-13 is due to changes in insolation, and that a warmer IPWP largely enhances the precipitation only in southern China. Moreover, such a role of warmer IPWP does not happen solely through its SST increase but via its synergic effect with insolation. Therefore, a warmer IPWP helps to explain the exceptional MIS-13 EASM precipitation in southern China as indicated in the paleo-red-soil records, but it does not help to explain it in northern China as recorded in the loess-soil sequences.

As the insolation of MIS-13 has not been found exceptional as compared to other interglacials (Yin and Berger, 2012), we need to seek other explanations for the exceptional EASM in northern China. This requires a better constraint of the spatiotemporal characteristics of the MIS-13 climate from geological records. The sea surface conditions over the Indian–Pacific oceans must be paid more attention because of their importance on the EASM and also because of many reconstruction uncertainties over these regions. For example, Mohtadi et al. (2006) hypothesized El Niño-like conditions during MIS-13, conditions which have been found in modern time associated with less summer rainfall in both southern and northern parts of China, and more rainfall in central China, around the lower reaches of the Yangtze River and the Huaihe River valleys (Zhang et al., 1999). By contrast, climate simulations show that MIS-13 was subject to a La Niña-like mean climatic state (Karami et al., 2014). More SST reconstructions from the tropical Pacific would help to understand better the ENSO situation during MIS-13 and its possible role on the EASM. In addition, the land ice sheet configuration of MIS-13 deserves more investigation because it could influence the East Asian climate through teleconnections. Many terrestrial records from the Northern Hemisphere indicate quite warm land surface during MIS-13 (Guo et al., 2009). Moreover, the pollen records from marine sediment of southwest Greenland show that MIS-13 has the second largest pollen abundance (only secondary to MIS-11) among the interglacials of the last 1 million years, leading to the assumption of the presence of forest vegetation at least over southern Greenland and a reduced Greenland ice volume (de Vernal and Hillaire-Marcel, 2008). In the meantime, the loess grain size data from northern China have indicated that MIS-13 had the weakest winter monsoon among the last nine interglacials (Guo et al., 2009). Therefore, the impact of a smaller Greenland ice sheet might be investigated in the future to see if it helps to explain the exceptional EASM precipitation in northern China as well as the weakened winter monsoon during MIS-13.

Acknowledgements. This work as well as Umesh Kumar Singh is supported by the European Research Council Advanced Grant EMIS (no. 227348 of the programme "Ideas"). Q. Z. Yin is supported by the Belgian National Fund for Scientific Research (F. R. S.-FNRS). The authors thank CISM staff at Université catholique de Louvain for technical support. Access to computer facilities was made easier through sponsorship from S. A. Electrabel, Belgium.

Edited by: D. Fleitmann

References

Berger, A.: Long-term variations of daily insolation and Quaternary climate changes, J. Atmos. Sci., 35, 2362–2367, 1978.

Berger, A.: The role of CO_2, sea-level and Vegetation during the Milankovitch-forced glacial-interglacial cycles, in: Proc. Geosphere-Biosphere Interactions and Climate, Cambridge University Press, 2001.

Braconnot, P., Marzin, C., Grégoire, L., Mosquet, E., and Marti, O.: Monsoon response to changes in Earth's orbital parameters: comparisons between simulations of the Eemian and of the Holocene, Clim. Past, 4, 281–294, doi:10.5194/cp-4-281-2008, 2008.

Chen, F. H., Bloemendal, J., Zhang, P. Z., and Liu, G. X.: An 800 ky proxy record of climate from lake sediments of the Zoige Basin, eastern Tibetan Plateau, Palaeogeogr. Palaeocl., 151, 307–320, 1999.

Cheng, H., Zhang, P. Z., Spotl, C., Edwards, R. L., Cai, Y. J., Zhang, D. Z., Sang, W. C., Tan, M., and An, Z. S.: The climatic cyclicity in semiarid-arid central Asia over the past 500 000 years, Geophys. Res. Lett., 39, 1–5, 2012.

Chou, C.: Land–sea heating contrast in an idealized Asian summer monsoon, Clim. Dyn., 21, 11–25, 2003.

Claussen, M., Mysak, L. A., Weaver, A. J., Crucifix, M., Fichefet, T., Loutre, M.-F., Weber, S. L., Alcamo, J., Alexeev, V. A., Berger, A., Calov, R., Ganopolski, A., Goosse, H., Lohman, G., Lunkeit, F., Mokhov, I. I., Petoukhov, V., Stone, P., and Wang, Z.: Earth system models of intermediate complexity: Closing the gap in the spectrum of climate system models, Clim. Dynam., 18, 579–586, 2001.

Crucifix, M. and Loutre, M. F.: Transient simulations over the last interglacial period (126–115 kyr BP): feedback and forcing analysis, Clim. Dynam., 19, 417–433, 2002.

de Garidel-Thoron, T., Rosenthal, Y., Bassinot, F., and Beaufort, L.: Stable sea surface temperatures in the western Pacific Warm Pool over the past 1.75 million years, Nature, 433, 294–298, 2005.

De Vernal, A. and Hillaire-Marcel, C.: Natural variability of Greenland climate, vegetation, and ice volume during the past million years, Science, 320, 1622–1625, 2008.

Duan, A. M., Sui, C., and Wu, G. X.: Simulation of local air-sea interaction in the great warm pool and its influence on Asian monsoon, J. Geophys. Res., 113, D22105, doi:10.1029/2008JD010520, 2008.

Fasullo, J. and Webster, P. J.: Warm Pool SST variability in relation to the surface energy balance, J. Clim., 12, 1292–1305, 1999.

Guo, Z. T., Liu, T. S., Fedoroff, N., Wei, L. Y., Ding, Z. L., Wu, N. Q., Lu, H. Y., Jiang, W. Y., and An, Z. S.: Climate extremes in Loess of China coupled with the strength of Deep- Water Formation in the North Atlantic, Global Planet. Change, 18, 113–128, 1998.

Guo, Z. T., Berger, A., Yin, Q. Z., and Qin, L.: Strong asymmetry of hemispheric climates during MIS-13 inferred from correlating China loess and Antarctica ice records, Clim. Past, 5, 21–31, doi:10.5194/cp-5-21-2009, 2009.

Ho, C. R., Yan, X. H., and Zheng, Q. N.: Satellite-observations of upper-layer variabilities in the Western Pacific Warm Pool, Bull. Am. Meteorol. Soc., 76, 669–679, 1995.

Huang, R. H. and Sun, F. Y.: Impact of the tropical western Pacific on the East Asian summer monsoon, J. Meteor. Soc. Japan, 70, 243–256, 1992.

Jouzel, J., Masson-Delmotte, V., Cattani, O., Dreyfus, G., Falourd, S., Hoffmann, G., Minster, B., Nouet, J., Barnola, J. M., Chappellaz, J., Fischer, H., Gallet, J. C., Johnsen, S., Leuenberger, M., Loulergue, L., Luethi, D., Oerter, H., Parrenin, F., Raisbeck, G., Raynaud, D., Schilt, A., Schwander, J., Selmo, E., Souchez, R., Spahni, R., Stauffer, B., Steffensen, J. P., Stenni, B., Stocker, T. F., Tison, J. L., Werner, M., and Wolff, E. W.: Orbital and Millennial Antarctic Climate Variability over the Past 800 000 Years, Science, 317, 793–796, 2007.

Karami, M. P., Herold, N., Berger, A., Yin, Q. Z., and Muri, H.: State of the tropical Pacific Ocean and its enhanced impact on precipitation over East Asia during Marine Isotopic Stage 13, Clim. Dynam., accepted, doi:10.1007/s00382-014-2227-0, 2014.

Kawamura, R., Matsuura, T., and Iizuka, S.: Role of equatorial asymmetric sea surface temperature anomalies in the Indian Ocean on the Asian summer monsoon and El Nino–southern oscillation coupling, J. Geophys. Res., 106, 4681–4693, 2001.

Kuang, X.-Y. and Zhang, Y.-C.: Impact of the position abnormalities of East Asian subtropical westerly jet on summer precipitation in middle-lower reaches of Yangtze River, J. Plateau Meteor., 25, 382–389, 2006.

Kubatzki, C., Montoya, M., Rahmstorf, S., Ganopolski, A., and Claussen, M. Comparison of the last interglacial climate simulated by a coupled global model of intermediate complexity and an AOGCM, Clim. Dynam., 16, 799–814, 2000.

Kukla, G., An, Z. S., Melice, J. L., Gavin, J., and Xiao, J. L.: Magnetic susceptibility record of Chinese Loess, Trans. R. Soc. Edinb. Earth Sci., 81, 263–288, 1990.

Kurihara, K.: A climatological study on the relationship between the Japanese summer weather and the subtropical high in the western northern Pacific, Geophys. Mag., 43, 45–104, 1989.

Lang, N. and Wolff, E. W.: Interglacial and glacial variability from the last 800 ka in marine, ice and terrestrial archives, Clim. Past, 7, 361–380, doi:10.5194/cp-7-361-2011, 2011.

Lau, K.-M., Kim, K.-M., and Yang, S.: Dynamical and boundary forcing characteristics of regional components of the Asian summer monsoon, J. Climate 13, 2461–2482, 2000.

Lee, E., Chase, T. N., and Rajagopalan, B.: Seasonal forecasting of East Asian summer monsoon based on the oceanic heat sources, Int. J. Climatol., 28, 667–678, 2008.

Li, C., Mu, M., and Zhou, G.: The variation of Warm Pool in the equatorial western Pacific and its impacts on climate, Adv. Atmos. Sci., 16, 378–394, 1999.

Liang, X. Z. and Wang, W. C.: Association between China monsoon rainfall and tropospheric jets, Quart. J. Roy. Meteor. Soc., 124, 2597–2623, 1998.

Liu, Y. M., Wu, G. X., Hong, J. L., Dong, B. W., Duan, A. M., Bao, Q., and Zhou, L. J.: Revisiting Asian monsoon formation and change associated with Tibetan Plateau forcing: II. Change, Clim. Dyn., 39, 1185–1193, 2012.

Lu, R. Y.: Interannual variability of the summer time North Pacific subtropical high and its relation to atmospheric convection over the Warm Pool, J. Meteor. Soc. Japan, 79, 771–783, 2001.

Luthi, D., Le Floch, M., Bereiter, B., Blunier, T., Barnola, J. M., Siegenthaler, U., Raynaud, D., Jouzel, J., Fischer, H., Kawamura, K., and Stocker, T. F.: High-resolution carbon dioxide concentration record 650 000–800 000 years before present, Nature, 453, 379–382, 2008.

Martin, G. M., Arpe, K., Chauvin, L. Ferranti, Maynard, L. K., Polcher, J., Stephenson, D. B., and Tschuck, P.: The simulation of the Asian summer monsoon in five European general circulation models, Atmos. Sci. Lett., 1, 37–55, doi:10.1006/asle.2000.0004, 2000.

Medina-Elizalde, M. and Lea, D. W.: The Mid-Pleistocene transition in the tropical Pacific, Science, 310, 1009–1012, 2005.

Mohtadi, M., Hebbeln, D., Ricardo, S. N., and Lange, C. B.: El Nino-like pattern in the Pacific during marine isotope stages (MIS) 13 and 11?, Paleoceanography, 21, PA1015, doi:10.1029/2005PA001190, 2006.

Muri, H., Berger, A., Yin, Q. Z., Voldoire, A., Salas, D., and Sundaram, S.: SST and ice sheet impacts on the MIS–13 climate, Clim. Dynam., 39, 1739–1761, 2012.

Muri, H., Berger, A., Yin, Q. Z., Karami, M., and Barriat, P.: The climate of the MIS-13 interglacial according to HadCM3, J. Climate, 26, 9696–9712, 2013.

Nitta, T.: Convective activities in the tropical western Pacific and their impact on the northern hemisphere summer circulation, J. Meteor. Soc. Japan, 65, 373–390, 1987.

Pope, V. D., Gallani, M. L., Rowntree, P. R., and Stratton, R. A.: The impact of new physical parameterizations in the Hadley Centre climate model: HadAM3, Climate Dyn., 16, 123–146, 2000.

Saji, N. H. and Yamagata, T.: Possible impacts of Indian Ocean Dipole mode events on global climate, Clim. Res., 25, 151–169, 2003.

Sardeshmukh, P. D. and Hoskins, B. J.: The generation of global rotational flow by steady idealized tropical divergence, J. Atmos. Sci., 45, 1228–1251, 1988.

Shen, S. and Lau, K.-M.: Bienniel oscillation associated with the East Asian summer monsoon and tropical sea surface temperatures, J. Meteor. Soc. Japan, 73, 105–124, 1995.

Shi, Z., Liu, X., and Cheng, X.: Anti-phased response of northern and southern East Asian summer precipitation to ENSO modulation of orbital forcing, Quat. Sci. Rev., 40, 30–38, 2012.

Shyu, J.-P., Chen, M.-B., Shieh, Y.-T., and Huang, C. K.: A Pleistocene paleoceano-graphic record from the north slope of the Spratly Islands, southern SouthChina Sea, Mar. Micropal., 42, 61–93, 2001.

Stein, U. and Alpert, P.: Factor separation in numerical simulations, J. Atmos. Sci., 50, 2107–2115, 1993.

Sundaram, S., Yin, Q. Z., Berger, A., and Muri, H.: Impact of ice sheet induced North Atlantic Oscillation on East Asian Summer Monsoon during an interglacial 500 000 years ago, Clim. Dyn., 39, 1093–1105, 2012.

Tschuck, P., Chauvin, F., Dong, B., and Arpe, K.: Impact of sea-surface temperature anomalies in the equatorial Indian Ocean and western Pacific on the Asian summer monsoon in three general circulation models, Int. J. Climatol., 24, 181–191, 2004.

Webster, P. J. and Lukas, R.: TOGA COARE: The coupled ocean atmosphere response experiment, Bull. Am. Meteorol. Soc., 73, 1377–1416, 1992.

Wei, J. and Wang, H.: A Possible Role of Solar Radiation and Ocean in the Mid-Holocene East Asian Monsoon Climate, Adv. Atmos. Sci., 21, 1–12, 2004.

Wei, G. J., Deng, W. F., Liu, Y., and Li, X. H.: High-resolution sea surface temperature records derived from foraminiferal Mg/Ca ratios during the last 260 ka in the northern South China Sea, Palaeogeogr. Palaeoclimatol. Palaeoecol., 250, 126–138, 2007.

Yang, F., and Lau, K. M.: Trend and variability of China precipitation in spring and summer: linkage to sea-surface temperatures, Int. J. Climatol., 24, 1625–1644, 2004.

Yin, Q. Z. and Guo, Z. T.: Mid-Pleistocene vermiculated red soils in southern China as an indication of unusually strengthened East Asian monsoon, Chinese Sci. Bull., 51, 213–220, 2006.

Yin, Q. Z. and Guo, Z. T.: Strong summer monsoon during the cool MIS-13, Clim. Past, 4, 29–34, 2008, http://www.clim-past.net/4/29/2008/.

Yin, Q. Z. and Berger, A.: Individual contribution of insolation and CO_2 to the the interglacial climates of the past 800 000 years, Clim. Dynam., 38, 709–724, 2012.

Yin, Q. Z., Berger, A., Driesschaert, E., Goosse, H., Loutre, M. F., and Crucifix, M.: The Eurasian ice sheet reinforces the East Asian summer monsoon during the interglacial 500 000 years ago, Clim. Past, 4, 79–90, 2008, http://www.clim-past.net/4/79/2008/.

Yin, Q. Z., Berger, A., and Crucifix, M.: Individual and combined effects of ice sheets and precession on MIS-13 climate, Clim. Past, 5, 229–243, doi:10.5194/cp-5-229-2009, 2009.

Yu, Pai-Sen and Chen, Min-Te.: A prolonged warm and humid interval during marine isotope stage 13–15 as revealed by hydrographic reconstructions from the South China Sea (IMAGES MD972142), J. Asian Earth Sci., 40, 1230–1237, 2011.

Zhang, R. H., Akimasa, S., and Masahide, K.: A diagnostic study of the impact of El Niño on the precipitation in China, Adv. Atmos. Sci., 16, 229–241, 1999.

Zhang, Z. Y., Gong, D. Y., He, X. Z., Gou, D., and Feng, S. H.: Reconstruction of the western Pacific Warm Pool SST since 1644 AD and its relation to precipitation over East China, Sci. China-Earth Sci., 52, 1436–1446, 2009.

Zhao, Y., Chen, Y., and Wu, A.: Sudden transition in the western tropical Pacific Warm Pool and its climatic effects, in: ENSO Monitoring and Predicting Studies, edited by: Zhai, P. M., Meteorological Press, Beijing, 78–85, 2000.

Zhou, T., Yu, R., Zhang, J., Drange, H., Cassou, C., Deser, C., Hodson, D., Sanchez-Gomez, E., Li, J., Keenlyside, N., Xin, X., and Okumura, Y.: Why the Western Pacific subtropical high has extended westward since the late 1970s, J. Climate, 22, 2199–2215, 2009.